

Large Microchannel Array Fabrication and Results for DNA Sequencing

Steve P. Swierkowski, Joseph W. Balch
Larry R. Brewer, Alex C. Copeland
J. Courtney Davidson, J. Patrick Fitch
Joseph R. Kimbrough, Ramakrishna S. Madabhushi
Ron L. Pastrone, Paul M. Richardson
Lisa A. Tarte, Marina Vainer

This paper was prepared for submittal to the
Micro-and Nanofabricated Structures and Devices for Biomedical Environmental
Applications II, SPIE's BiOS '99 International Biomedical Optics Symposium
San Jose, CA
January 23-29, 1999

January 7, 1999



This is a preprint of a paper intended for publication in a journal or proceedings.
Since changes may be made before publication, this preprint is made available with
the understanding that it will not be cited or reproduced without the permission of the
author.

DISCLAIMER

This document was prepared as an account of work sponsored by an agency of the United States Government. Neither the United States Government nor the University of California nor any of their employees, makes any warranty, express or implied, or assumes any legal liability or responsibility for the accuracy, completeness, or usefulness of any information, apparatus, product, or process disclosed, or represents that its use would not infringe privately owned rights. Reference herein to any specific commercial product, process, or service by trade name, trademark, manufacturer, or otherwise, does not necessarily constitute or imply its endorsement, recommendation, or favoring by the United States Government or the University of California. The views and opinions of authors expressed herein do not necessarily state or reflect those of the United States Government or the University of California, and shall not be used for advertising or product endorsement purposes.

Large microchannel array fabrication and results for DNA sequencing

Steve P. Swierkowski, Joseph W. Balch, Larry R. Brewer, Alex C. Copeland, J. Courtney Davidson,
J. Patrick Fitch, Joseph R. Kimbrough, Ramakrishna S. Madabhushi, Ron L. Pastrone,
Paul M. Richardson, Lisa A. Tarte, Marina Vainer

Lawrence Livermore National Laboratory, MS L-222, 7000 East Avenue, Livermore, CA, 94550

ABSTRACT

We have developed a process for the production of microchannel arrays on bonded glass substrates up to 14 x 58 cm, for DNA sequencing. Arrays of 96 and 384 microchannels, each 46 cm long have been built. This technology offers significant advantages over discrete capillaries or conventional slab-gel approaches. High throughput DNA sequencing with over 550 base pairs resolution has been achieved. With custom fabrication apparatus, microchannels are etched in a borosilicate substrate, and then fusion bonded to a top substrate 1.1 mm thick that has access holes formed in it. SEM examination shows a typical microchannel to be 40 x 180 micrometers by 46 cm long; the etch is approximately isotropic, leaving a key undercut, for forming a rounded channel. The surface roughness at the bottom of the 40 micrometer deep channel has been profilometer measured to be as low as 20 nm; the roughness at the top surface was 2 nm. Etch uniformity of about 5% has been obtained using a 22% vol. HF / 78% Acetic acid solution. The simple lithography, etching, and bonding of these substrates enables efficient production of these arrays and extremely precise replication from master masks and precision machining with a mandrel.

Keywords: microchannels, microchannel plates, DNA sequencing, electrophoresis, borosilicate glass

1. INTRODUCTION

Electrophoresis may be defined as the differential drift velocity movement of electrically charged chemical ion or molecular species under the force applied by an electric field in a fluidic separation medium. Early work by Tiselius on protein separation by electrophoresis was introduced in 1937 and for this pioneering electrophoresis work with large tubes, he received the Nobel prize. Limitations arising from diffusion and convection has led to the use of polyacrylamide or agarose sieving media in the separation channel in many instruments, including the popular slab gel type. Large improvements in separation performance were introduced with the use of very narrow (75 μ m) bore fused silica capillaries in the 1980s. However the slab gel instruments have the advantage of running many samples in parallel, in spite of practical difficulties in slab gel plate preparation, sample injection, and lane tracking. Fused silica capillaries with inner coating and electrokinetic sample injection have produced some very good sequencing results¹. These high resolution capillaries are very small and not as robust or strong as larger separation structures, and care must be taken in high pressure sieving media filling and fixture design for both sieving media filling and sample injection. Early work with microchannels etched in flat glass substrates^{2,4}, versus drawn glass capillaries, indicated the potential of chemical separation done with the methodology of micromachining. In this work we distinguish our very long, narrow bore separation tubes, with one sample per channel, as microchannels, versus drawn capillaries. In order to meet the high throughput needs of DNA sequencing, our microchannels are fabricated as large planar arrays in borosilicate float glass⁵ that is primarily made up of fused silica; it contains other oxides that results in a lower softening point, is much less expensive than fused silica plates, and yet is extremely rugged to mechanical and thermal stresses and is also chemically resistant. Our microchannel arrays are fabricated in two borosilicate substrates that are fusion bonded together into one microchannel plate; this plate may be cleaned or regenerated only by pumping chemicals and sieving media into a single slot manifold port on the output end of the plate.

The fabrication approach we have taken is to adapt existing advanced flat panel display type resources, processes and procedures. The fabrication also benefits from the quality that is enabled by performing critical steps in a Class 100 clean room environment. This method allows rapid changes in microchannel array design, since it is entirely based on commercial photomask sources that directly use our custom designs done with standard CAD software tools. Some of the processing can be done with batches of parts such as metal etch mask coating and substrate cleaning. The top glass substrate with the access ports is very precisely ultrasonically milled at a commercial source⁶ with a master mandrel tool that again, assures economical, exact replication of one of the just two substrates needed to make the final microchannel array. Basic lithographic contact printing of the channel array pattern is done with a very simple and inexpensive custom built photoresist

dip coater apparatus and an easily modified commercial UV flood source. For limited production, this avoids the high cost and maintenance of a full flat panel photoresist coating tool and non-contact lithography exposure tool.

Microchannel electrophoresis arrays share many of the benefits of capillary arrays such as: short separation times, no lane tracking required, sieving media pumped directly into the array, and resolution of over 500 bases. Furthermore, our microchannel arrays have several additional positive attributes:

- The integrated array of microchannels in a single fused plate is very robust.
- Only two components are fabricated and bonded to make an array plate, greatly reducing handling of discrete parts.
- Sieving media fill or replenishment is done with a single O ring sealed port.
- A planar optical window and a precision planar array enable efficient laser fluorescence detection, with built in planar fiducial alignment.
- The channel shape is wide and shallow of depth, optimizing both sieving media heat dissipation and the detection signal.
- The microchannel array design is easy to change with CAD tools, and the fabrication method can handle diverse structures such as single ended loads, T loads, and the addition of in-plane fiducial features, or electrodes in the channel.
- A micrometer precision lithographic fabrication mask enables very high linear density of channels.
- The extremely precise (1 μm) lithographic patterning allows one to add other features to the microchannel substrate for optical fiducials and robotics loading fiducials that are built in, greatly simplifying system assembly. The most crucial interfaces of the microchannel plate to the rest of the system are self registered.
- It is economical to produce exact replica plates with reusable photomasks and a simple fabrication process.

2. DESIGN

Microchannel array fabrication starts with the design of the photomask using standard CAD layout tools. The finished design can be electronically transferred to commercial photomask companies. The laser pattern generator has one micrometer resolution, but most of the design features we are using are 20-100 micrometers wide, which are very large by common photolithography standards. This translates to easy contact photolithography and highly defect tolerant process parameters. Since the processing requires a clear-features, dark-chrome on soda-lime glass mask, it is critical that the channel lines not have any chrome mask shorts or bridges. This may require a small number of defect removals with laser ablation to produce a defect free master mask. Since our lithography patterns are rectangular, e.g. up to 14 x 51 cm in size, several different designs can fit on one standard sized 45 x 55 cm photomask blank. It is easier to tolerate a few inevitable pinholes in a dark field (i.e. negative) mask, because with the choice of a positive photoresist, a mask pinhole in the background field transfers into an etch pit in the unpatterned field of the glass, and this is just bonded into the glass and doesn't affect the microchannels.

Chrome-gold etch masks are commonly used in micromachining. Most etching processes amenable to large glass substrates etched up to a depth of 100 μm are HF-based and this requires a very durable pinhole free etch mask. This extremely low defect rate metal etch mask layer can be obtained by using physical vapor deposition (PVD) in a high quality large vacuum system. Since the glass substrates are much longer than wide, it is economical to metal coat several substrates at once in the large diameter coating system. A custom designed vacuum substrate carrier that can accommodate three to six substrates simultaneously is used.

A variety of methods can be used to deposit the photoresist on the metal coated glass substrates. These include roller coating, spray coating, meniscus coating, electrodeposition, and dip coating. The commonly used spin coating in micromachining is not practical for substrates of this size and shape. There are many tradeoffs for these different methods, but dip coating seemed easiest to implement for the very thick (6-8 μm), low defect, highly durable positive resist used which is designed for dip coating. A simple custom made dip coating apparatus is shown in Fig. 1. It's key features are extremely low vibration (high mass base), a slow, extremely stable pull rate of about 2.5 cm/min (precision lead screw driven), and an interchangeable dip tank. Typical photoresist coatings with this apparatus are about 7 μm thick with visible thickness fringes smoothly spread out over several centimeters longitudinally. The lateral thickness variations are typically less than a fringe. This is important to obtain uniform lithography feature size.

An excellent way to expose the resist is with a non-contact scanning source exposure tool. This can scan the whole photomask and since it avoids contact to the substrate, particulate mask damage is less likely - especially for a high throughput fabrication. However, these tools are very expensive (many hundreds of K\$). Since the microchannel arrays are much narrower than the whole photomask, we can use a much less expensive exposure tool by adapting a common 15 cm square UV flood source (~20 K\$). This is done by using contact printing and pulling the mask/substrate pair under the flood

source field on a scanning mechanical track. This scan exposure tool is shown in Fig. 2 and it takes less than 10 minutes to scan a substrate.

We have designed and built a wide variety of microchannel array structures with this process method. These include: a.) T load structures with 3 input ports per channel, b.) a set of different width channels with a single input and output port, c.) sets of channels with single port inputs and one manifold slot output port; 12 or 24 or 96 or 384 channels on a single plate. These designs use ultrasonically drilled holes in the top substrate from 0.5-1.5 mm diameter, which are then aligned to the microchannel substrate for fusion bonding. One other very different input structure was built that used a precision saw slot input port that then was backside patterned with a lithographic, chemically-etched small injection hole. This small hole was etched into the bond side of the top substrate; it was then aligned onto the end of the microchannel in the bottom substrate for bonding. All these different array types and structures were made with just two master large photomasks. It is very attractive to have design variations easily changed, have many of them on one CAD mask layout, and have the precision and parallelism that micromachining and photolithography provide.

3. FABRICATION

The fabrication of the microchannel bottom substrate starts with PVD coating of the 5 mm thick borosilicate glass on the float-up side with 30 nm of Cr, followed by 1 μm of Au, as shown schematically in Fig. 3. The chrome is required for adhesion. The gold is extra thick to prevent pinholes and to provide a compliant but reasonably strong overhanging portion of the metal mask as the glass etching will later undercut the etch mask by an amount almost as much as the etch depth. The patterned photoresist is left on the gold for the glass etch; it degrades substantially during the longer HF etches, but it still adheres well to the gold and provides very good mechanical support to the gold as the metal mask is undercut. The composite etch mask is so strong that the etch can be interrupted for checking depth, and then resumed without loss of the undercut etch mask lip; this entails a careful water rinsing of the plate and blow dry with nitrogen. After metal etch mask layers are deposited, the substrate is then dip coated in Shipley SP 20-29 positive photoresist to a thickness of about 7 μm . After UV exposure with contact printing, the photoresist is developed and it then has windows where the channel is to be etched. The gold is etched next and then the chrome, so that the net result is the photolithography photoresist pattern is transferred into the metal mask. The bottom of the substrate is coated with a plastic tape to prevent the glass etch from degrading the photoresist that is directly on the glass there, which would then result in non-uniform frosty etching of the substrate backside. This backside will eventually become the entry window for the optical detection system. The bottom glass substrate is then etched in a HF(22%vol)/Acetic Acid mixture with uniform moderate agitation. The etch rate is about 0.7 $\mu\text{m}/\text{minute}$, and a typical etch depth is about 45 μm . The glass etch is approximately isotropic, but tends to etch a little less underneath the mask overhang where it is close to the mask; the reaction product removal is a little less in this region, depending upon etch composition, rate, and convection. This slight etch anisotropy is very desirable because it produces a glass overhang or cusp in the bottom substrate; this then makes the interior of the final microchannel cross section smoothly concave. After the microchannel substrate is etched to the desired depth, the photoresist and metal etch mask are all stripped off, completing fabrication of the bottom microchannel substrate.

The 1.1 mm thick top substrate is patterned by ultrasonic machining⁶ to form the input hole ports and a common sieving media fill manifold slot. The top is bonded to a thick sacrificial support glass platform for this process with a low temperature wax, so that the drill mandrel will not chip away the edges of its pattern as it emerges through the top substrate. Various hole sizes from 0.5 to 1.5 mm have been drilled in glass ranging from 1.1 mm to 5.0 mm thick. The current 96 and 384 microchannel arrays use top hole substrates that are 1.1 mm thick bonded to bottom microchannel substrates that are 5.0 mm thick. The 96 hole top substrates use simple cylindrical 1.0 mm diameter holes. The 384 hole top substrates use a tapered square hole that is about 1 mm diameter at the top or outside, and about 0.5 mm diameter on the bond side. The smaller exit hole enables tighter packing density of microchannels at the bond interface. This enables 384 input wells to be placed on the standard 4.50 mm titer plate pitch with a 16 x 24 array; also, the 384 channel plate fits on the same footprint as the 96 channel plate. After stripping off the wax residues and carefully cleaning any particulates, the top substrate is completed.

The bonding process starts with a final cleaning and rinse of the two glass substrates. A final organic strip is done with a sulfuric acid / hydrogen peroxide etch, followed by a 10 minute rinse in DI water. The microchannel substrate and the hole substrate are placed together with some thin shims that are temporarily placed between the two substrates on their ends. The holes in the top substrate are aligned to the microchannels in the bottom substrate. The substrates are pressed together, the shims are removed, and the parts and their graphite platform are placed in a nitrogen furnace and fusion bonded at 660° C for 1 hour.

4. CHARACTERIZATION

The microchannel profile after the glass etch is completed appear in the SEM images shown in Figs. 4 and 5. The sample is at a very high tilt angle in the SEM, so the vertical direction is strongly foreshortened; this enables viewing the undercut

cusps in the glass and highlights the texture of the surfaces. For a typical etch depth of 40 μm , the surface roughness measured with a contact profilometer is about 20 nm at the bottom of the etch and the original float side surface is 2 nm rough before bonding. A vertical plan view of the edge of the microchannel is shown in Fig. 6. It shows the edge roughness of the cusp resulting from the combination of lithography edge definition, particulate defects and any impurities in the glass. It has a roughness of about one micrometer; this effect is visible in the exaggerated texture shown on the side wall of the image in Fig. 5. This is the long wavelength roughness visible with moderate resolution microscopy before bonding. After bonding, the atomic level smoothness is expected to be better after the annealing and initial surface reflow achieved at the bonding temperatures. The channel cross sectional shape after bonding is shown in Fig. 7. This clearly illustrates the smooth continuously curved inside shape of the microchannel. It also shows that for small features of this size that the top and bottom surfaces of the microchannel remain flat through the bond cycle. It is observed that the glass does become soft enough to sag or warp if the unsupported regions are millimeter in size. The high temperature profile of the bonding process very thoroughly anneals out the residual strain in the plate. Another measurement test on this same sample, was to cleave the plate across all the channels and examine the channels at the cleave, especially at the bond interface. The SEM image in Fig. 8. shows no trace of the bond interface; there are a few particles remaining from the cleaving procedure. There was no evidence of any bond interface delamination, or any other visible effect, for all the channels even after the extreme tensile stress experienced by cleaving.

The bonding platform must be very flat to keep the overall plate very flat through the bonding cycle. One crucial area for extreme flatness is along the plane of the microchannels in the optical readout zone. This was tested by taking a sawcut cross section of the microchannel array all the way across a 75 mm wide plate after bonding. A cleaved silicon wafer provides an atomically smooth straight edge reference part that is overlapped on the microchannel cross section under a high power optical microscope. The pair of parts was translated on the microscope stage and the separation between the channels and the silicon straight edge was measured to a precision of about 1 μm . The results showed the bonded microchannels along this lateral section to be planar within the experimental resolution of 1 μm over all the microchannels.

We have recently fabricated a 384 channel plate on a 14 x 58 cm substrate. Fifteen etch depths were measured over the entire 12 x 47 cm channel region. The average channel depth was 42.5 μm with a standard deviation of 1.06 μm ; however the estimated depth measurement precision was 1 μm . The data showed that there was no measurable depth variation laterally across the plate and that there was a small uniform decrease longitudinally along the plate. In other words, the channels all have the same shape. The average channel width was 122 μm and the estimated precision is 0.5 μm . There was no measurable systematic variation in channel width over the plate.

Plate defects can arise from several sources, and they may be sorted into two major categories: a.) those due to initial scratches or inclusions in the glass in its initial state, and b.) those that are acquired from process handling - and most of these appear to come from particulates, if scratches induced by processing are minimized with extremely careful technique and use of class 100 cleanroom procedures. The initial scratch damage in the glass can be so small as to not be visible under normal microscopic inspection. Indeed, it is easy to see subsurface damage resulting from optical quality polishing that leaves a smooth top surface but damaged bonds and strain tracks below the surface. The scratch tracks become evident as dagger shaped cuts into the microchannel sidewall; they have a straight keel and terminate in a very sharp point. This is a result of accelerated etching along the damage track. An accidental scratch of this type is shown in Fig. 9.; this type of scratch typically leaves a set of dagger shape partial cuts across several microchannels. Sometimes they have a straight trail of defects even along the unetched glass as shown in Fig. 9. The second and more common type of defect appears as a semicircular bite into the sidewall as shown in Fig. 10. This type of defect often has a somewhat hemispherical surface and looks like a smooth dent. It is most commonly seen in the glass between the patterned features and channels and is of no consequence. It is thought to be usually caused by a flaw in the photoresist - perhaps a small spot of poor adhesion, or a very small particle in the resist. It could also be a defect initially in or on the metal mask layer. We have recently made 96 channel plates with about 5 visually obvious defects per plate. Fortunately, some recent data has been obtained that shows that the vast majority of these defects have no effect on resolution of the sequenced data. Occasionally, a single defect or two might be big enough to cause two channels to short out laterally. These channels could easily be computationally excluded from the final data since they are fixed and known, and the plate lifetime is high enough to be unknown at this time.

We have pressure tested the plates two ways. First, the injection holes were closed off and water was applied at the output sieving media fill slot until failure. This occurred about halfway down the plate at about 300 psi. Since this test was done a year ago, we have improved the processing, the plate design, and the testing. Second, recent tests have been in a working sequencing instrument where sieving media replenishment has used pressures of over 500 psi. With many, many tests, no failures in plates has been observed. This is a more realistic test, since it is the way the device is used for sequencing and the pressure in the plate uniformly drops from a maximum at the slot end to zero at the input end.

5. RESULTS

Microchannel plates containing 96 channels have been used extensively over the past six months. One plate has been used more than 130 times, generating nearly 500,000 high quality base calls from various test samples. Depending on the purity of the samples we load into the system, we can use the plate 15 to 30 times before performance begins to degrade due to fouling of the channel walls. When this happens, the channels can be easily regenerated by in situ flushing with solvent followed by an acid etch and water rinse.

Samples are introduced into the channels through holes in the top plate. A small volume syringe is used to transfer the 100-500 nL required for analysis. We typically use commercially available gel loaders which contain 8 or 12 syringes for loading the plate. The sample input holes are arranged in an 8 x 12 array on 9 mm centers corresponding to the industry standard microtiter plate, so that we could easily use a 96 syringe device to load samples directly from a microtiter plate. After loading the wells, DNA is then electrokinetically loaded onto the microchannels and then drifts and separates under the influence of an applied electric field of 100 - 150 V/cm. Typical run times are 180 minutes which allow us to collect data from over 500 peaks per lane.

A lane map for a 96 microchannel plate is shown in Fig. 12. The titer plate input port format makes each row of channels 9 mm different in length. The longest channels are 418 mm to the optical readout; the shortest ones are 63 mm shorter. The microchannels are about 45 x 170 μm in cross section. The arrival time of the primer peaks shows a sawtooth pattern because of the different drift lengths, for the different input rows. The built in fiducial pattern is shown on the sides of the figure as two constant lanes on the left and three constant lanes on the right; they are etched with the same pitch as the microchannels. A sample of a raw electropherogram from a lane somewhere in the middle is shown in Figs. 13 and 14. One can clearly see the peak width and separation and good signal to noise ratio before smoothing and filtering. The peak width and adjacent peak spacing is shown in Fig. 15 as a function of approximate base number. This is frequently referred to as a crossover plot. This plot was generated by fitting Gaussians to the color and mobility corrected data for the peaks. There is some scatter in the data and the general trend is indicated by the solid curves that are quadratic fits to the data. They indicate the narrow constant peak widths that can be obtained as indicated in the lane map of Fig. 12.

6. CONCLUSIONS

We have developed a design and fabrication procedure for high density microfluidic arrays in borosilicate glass up to 58 cm in size that are easy to reproduce, inexpensive, and physically robust. This technology is suitable for many kinds of analytical instruments and combinatorial chemistry processes, such as microliter sized sample preparation involving very high sample numbers. If the separation path lengths can be used as short as 10 - 15 cm, then it is straightforward to place as many as 1,200 channels on one of our plates. At that scale, the current channel number limit seems to be from input injection port size and especially the technique used to load and transfer small samples. The common method of physically contacting and holding the microfluidic sample for transfer into an instrument or a sample tray is a major limitation. The promise of kinetic microdrop transfer through the air from microlithographic nozzle arrays to plates such as ours, other instrumentation, or sample trays is evident from the ubiquitous ink jet printer technology which can be adapted to biosamples and provide lineal input spatial densities commensurate with the microchannel density we have demonstrated.

We have demonstrated DNA sequencing with up to 550 base resolution in a 96 microchannel plate based system that has convenient in situ recycling and regeneration. Similar plates with 384 channels per plate have just been fabricated. Since the microchannel shape and size is very comparable, if adequate loading and injection can be performed, these plates should provide a high throughput system highly suitable for DNA sequencing.

ACKNOWLEDGMENTS

The authors acknowledge the support and funding provided by the NIH and DOE programs in human genomics and especially the unwavering support of the LLNL Biology and Biotechnology Research Program. The excellent quality large PVD metal film depositions by Steve Falabella, LLNL, is greatly appreciated. The flexible resource sharing and helpful suggestions of the staff of the LLNL Center for Microtechnology has made this effort possible.

REFERENCES

1. E. Carrilho, M. Ruiz-Martinez, J. Berka, I Smirnov, W. Goetzinger, A. Miller, D. Brady, B. Karger, *Anal. Chem.*, 68, pp. 3305-3313, 1996.
2. A. Manz et. al. , *J. Chromatogr.* 593, p. 253, 1992.
3. D. J. Harrison, et. al., *Anal. Chem.*, 64, p. 1926, 1992.
4. D. J. Harrison, et. al., "Micromachining a Miniaturized Capillary Electrophoresis-Based Chemical Analysis System on a Chip", *Science* 261, pp. 895-897, August 13, 1993.
5. BORO FLOAT™, Schott Corporation, Technical Glass Division, 3 Odell Plaza, Yonkers, N.Y. 10701.
6. Ultrasonic milling and mandrel by Bullen Ultrasonics, Inc., 4613 Camden Road, Eaton, Ohio 45320.

FIGURES

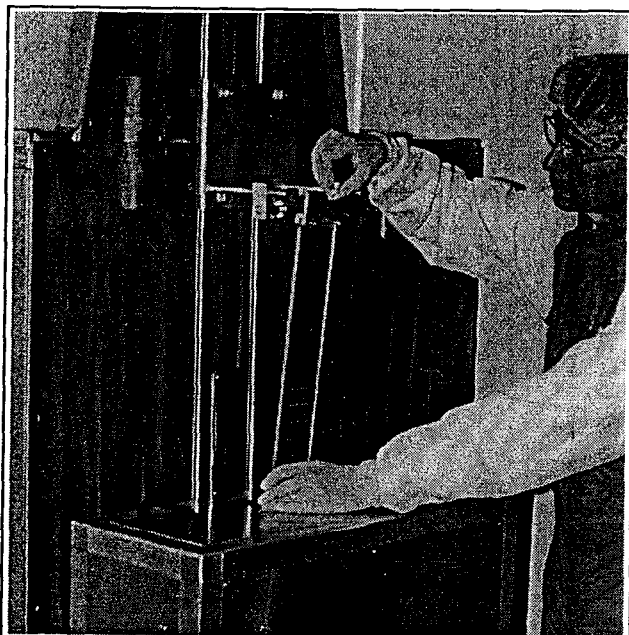


Fig. 1. The photoresist dip coating apparatus is on a stable low vibration floor in a class 100 cleanroom. It can accommodate plates up to 70 cm long. A 7.5 x 58 cm plate is shown being inserted. The top of the plate hangs on a fixture that travels up a precision vertical lead screw with very low vibration.

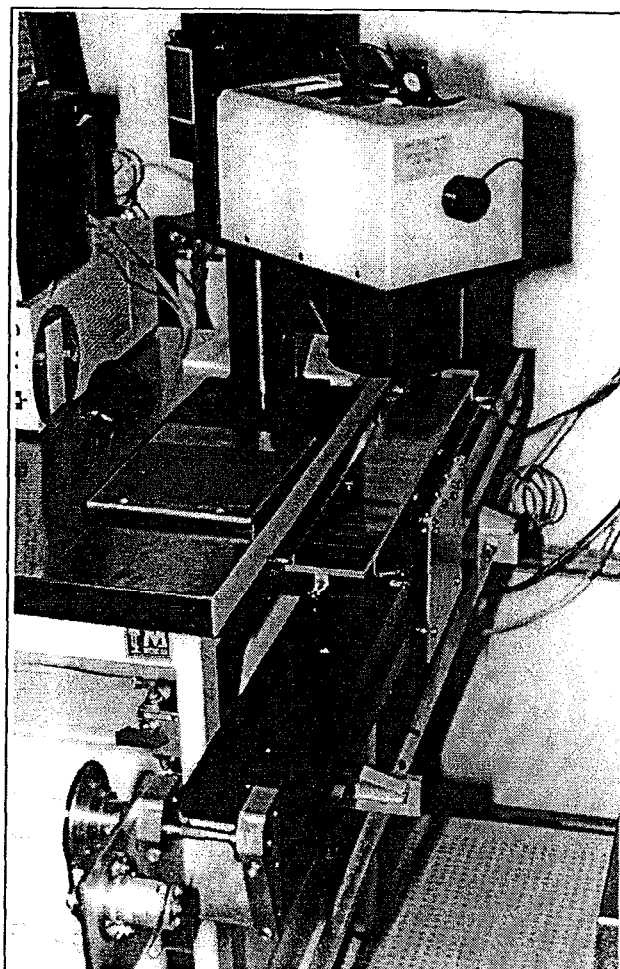
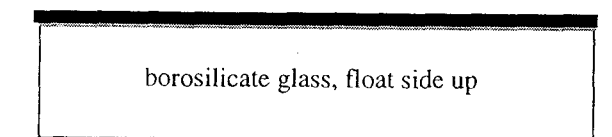
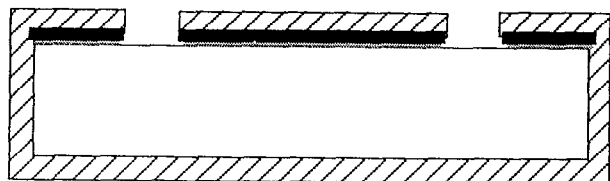


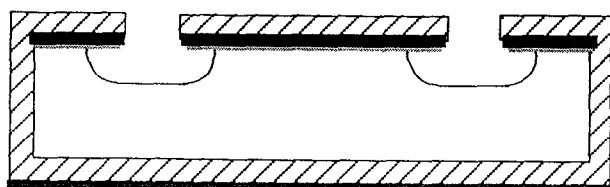
Fig. 2. The exposure system uses a standard small sized 405 nm UV flood source. It is shown above the mechanical track that pulls the mask/substrate clamped pair underneath the rectangular flood field, to provide a uniform exposure of substrates up to 70 cm long in about 10 minutes.



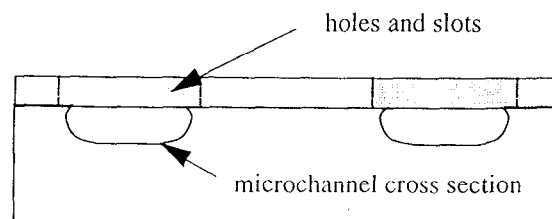
a.) coat 30 nm Cr, 1 μ m Au etch mask



b.) dip coat PR, pattern PR, Au, Cr



c.) coat bottom, HF etch



d.) align top glass with holes and slots, fusion bond

Fig. 3. The fabrication uses photolithography, metal etch masks, wet etching, ultrasonic machining, and fusion bonding.

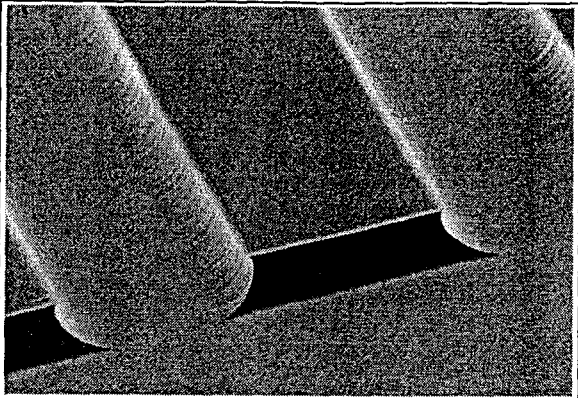


Fig. 4. An SEM image of microchannels before bonding that was made with a $50\text{ }\mu\text{m}$ wide metal etch mask that has been removed. The metal etch mask was under cut on each side by about the etch depth of $40\text{ }\mu\text{m}$ and the channel is about $130\text{ }\mu\text{m}$ wide, so the etch is nearly isotropic ($40+40+50=130$). The glass rib or mesa sidewalls have been etched on all sides and the corner flute is actually at 45 degrees to the channel, but does not appear so in this very oblique SEM image where the vertical direction on the sample is highly foreshortened.

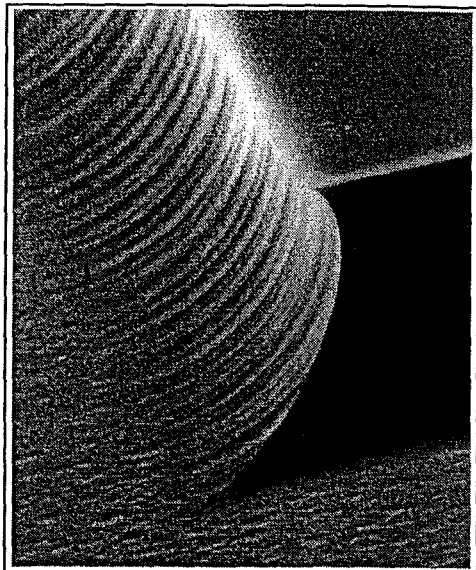


Fig. 5. The SEM image shows the $5\text{ }\mu\text{m}$ undercut lip is very sharp and smooth; this is needed to form a bonded microchannel with completely smooth concave corners on the interior and no interior seam or crack.

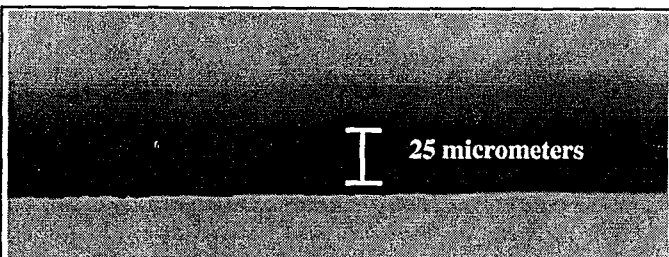


Fig. 6. A plan view optical photomicrograph of the edge of the undercut micro channel has an edge roughness about one micrometer.

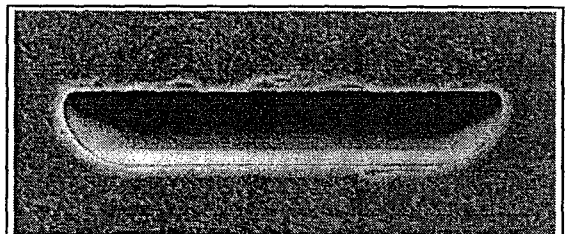


Fig. 7. The cross section view of a typical microchannel after bonding. The texture around the channel and chipping around the edges is from the diamond blade sawcut. The sawcut is planar and the very nearly end on view gives a true picture of the channel cross section shape. This channel is $30\text{ }\mu\text{m}$ deep and $176\text{ }\mu\text{m}$ wide. The bond plane is perpendicular to this image and coincident with the upper flat surface of this channel.



Fig. 8. A cleaved cross section of a channel shows a featureless fusion bond at the flat edge near the top of the image.

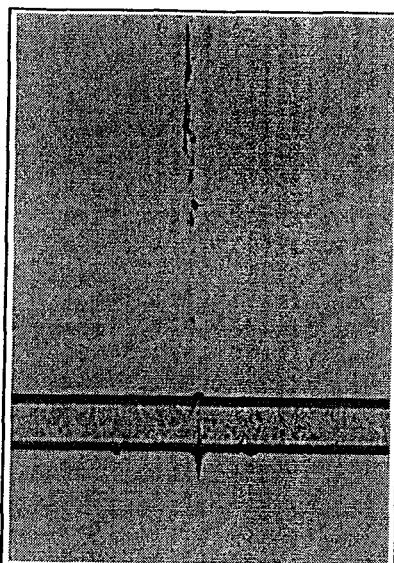


Fig. 9. Initial scratch in glass causes sharp lateral dagger defect in an etched microchannel.

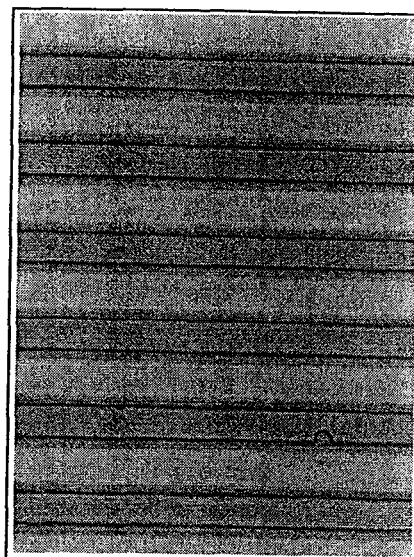


Fig. 10. A semicircular process defect in the first channel (white) at the bottom. The channel pitch is 300 μm .

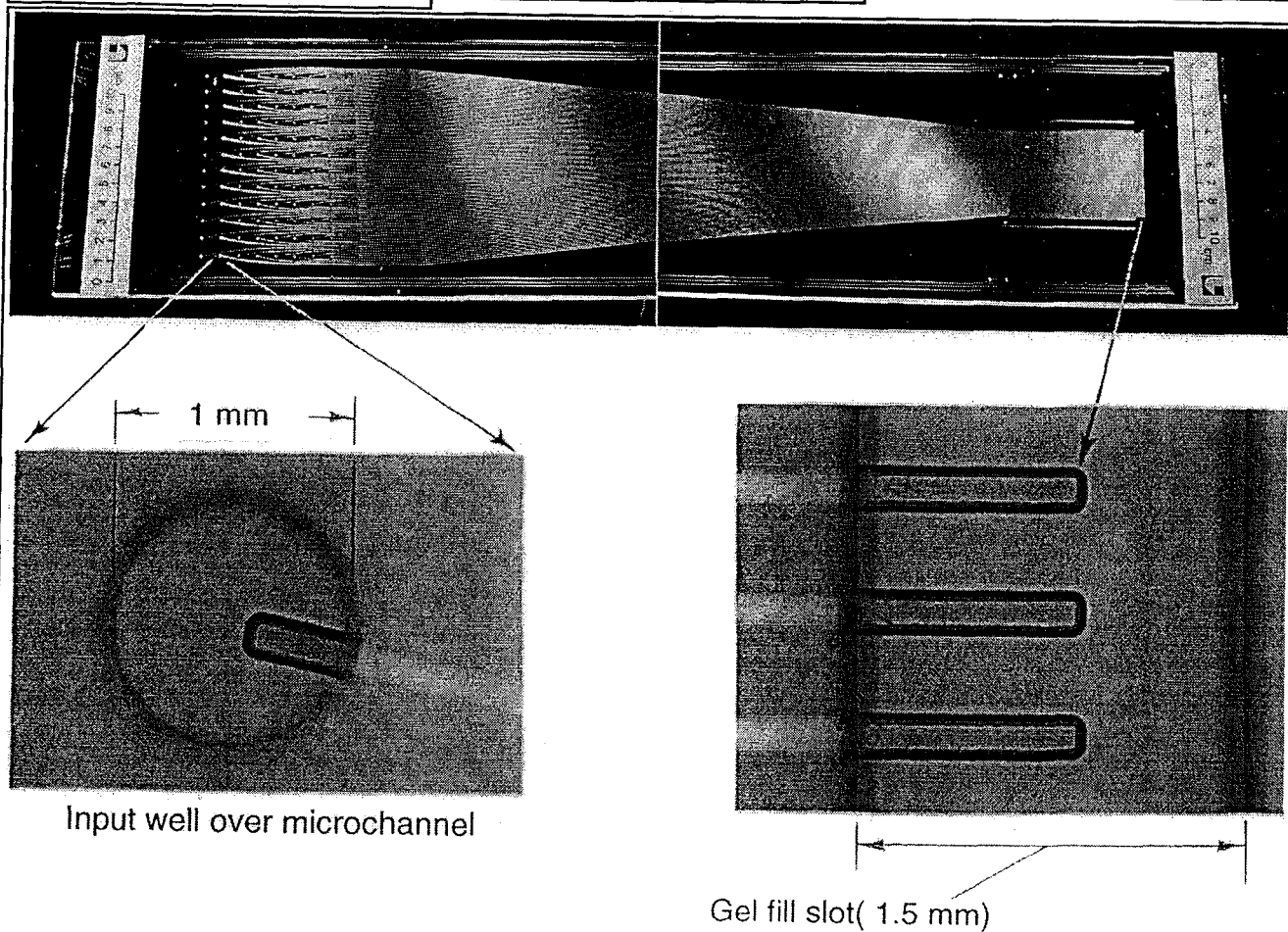


Fig. 11. The large image is a 96 microchannel array plate that is 14 cm x 58 cm long. The 8 x 12 titer format is visible on the left end where 8 x 12 input wells are on 9mm centers. The microchannels shown in the inset images are 46 cm long x 190 μm x 53 μm deep.

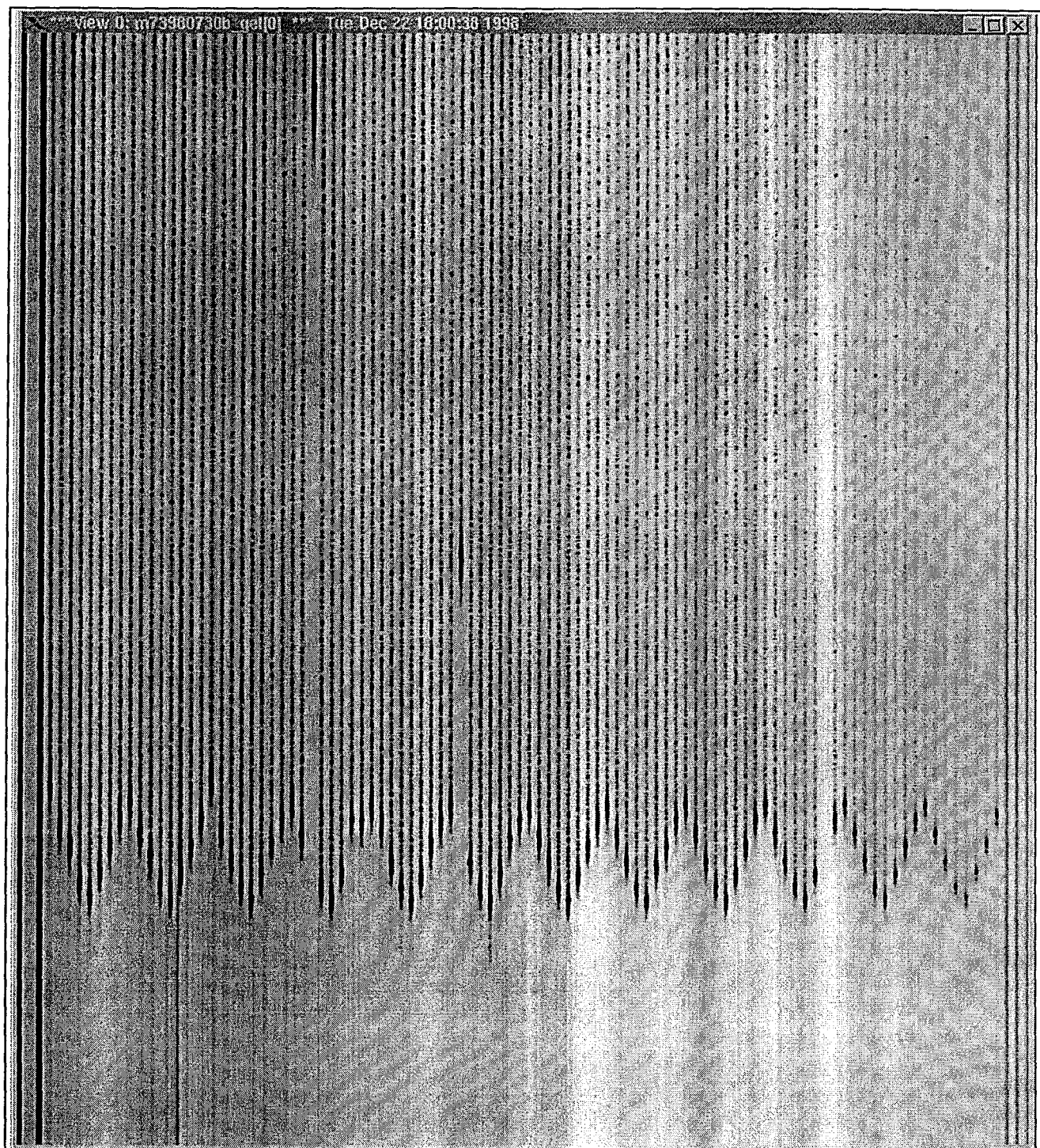


Fig. 12. Lane map showing all 96 microchannel lanes for the blue dye that labels the DNA base C. Scanning across the plate every second, the displayed data is collected in 2.5 hours (time origin at bottom), with an applied voltage of 4.8 kV. The sample is a energy transfer dye labeled M13 sequencing standard. The staggered arrival of the primer peaks is due to the microtiter format of the input wells resulting in slightly different length channels. Note the uniformity of separation across the microchannels. Three lanes in this example show anomalous behavior due to accidental load variation but produced good data on subsequent runs.

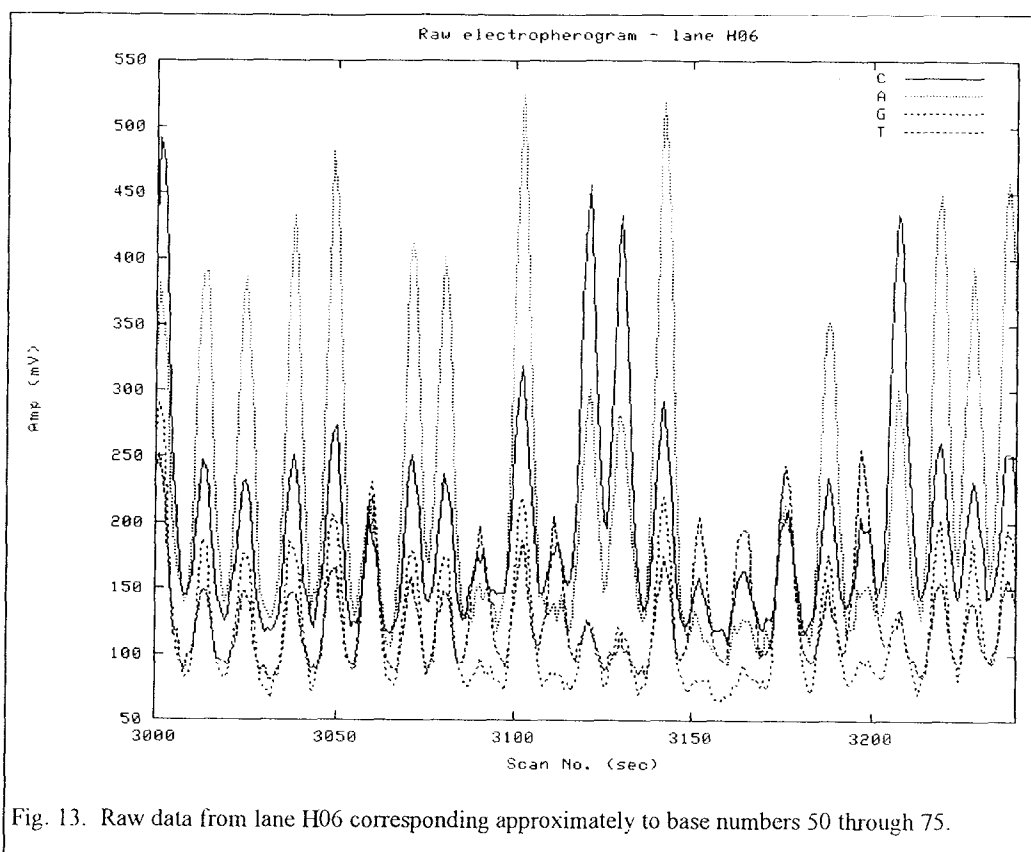


Fig. 13. Raw data from lane H06 corresponding approximately to base numbers 50 through 75.

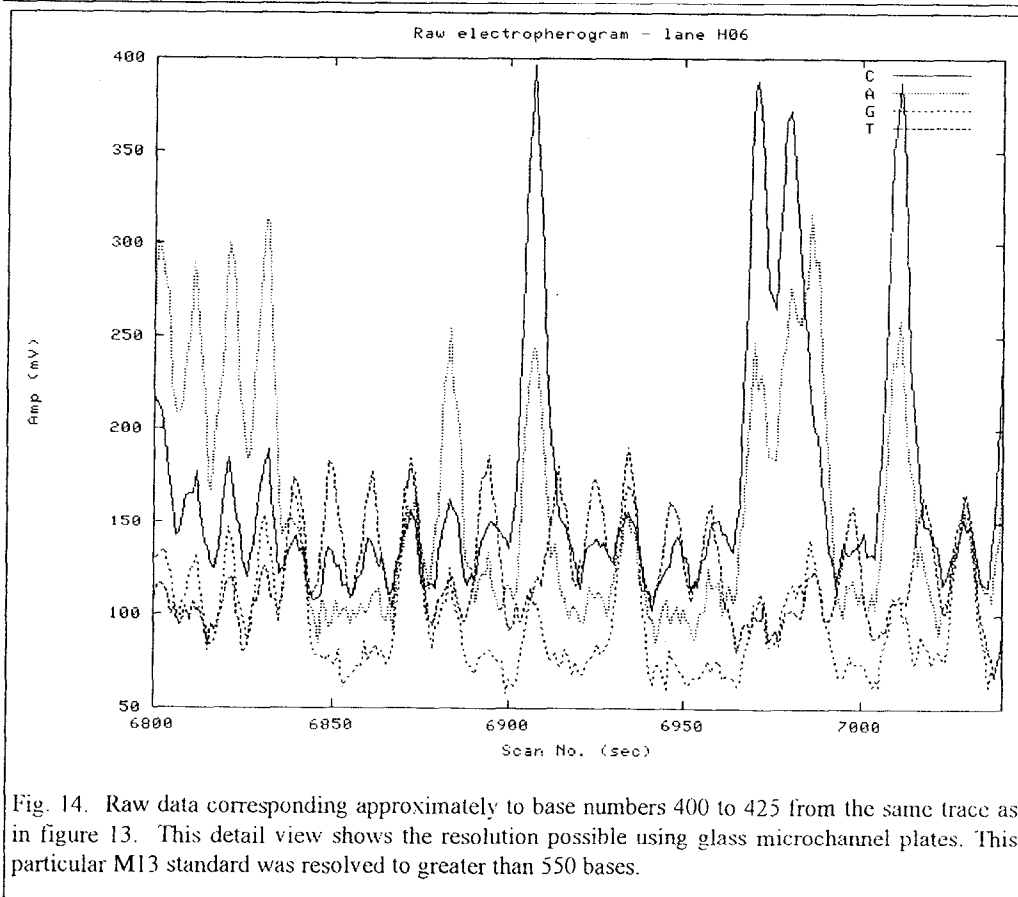


Fig. 14. Raw data corresponding approximately to base numbers 400 to 425 from the same trace as in figure 13. This detail view shows the resolution possible using glass microchannel plates. This particular M13 standard was resolved to greater than 550 bases.

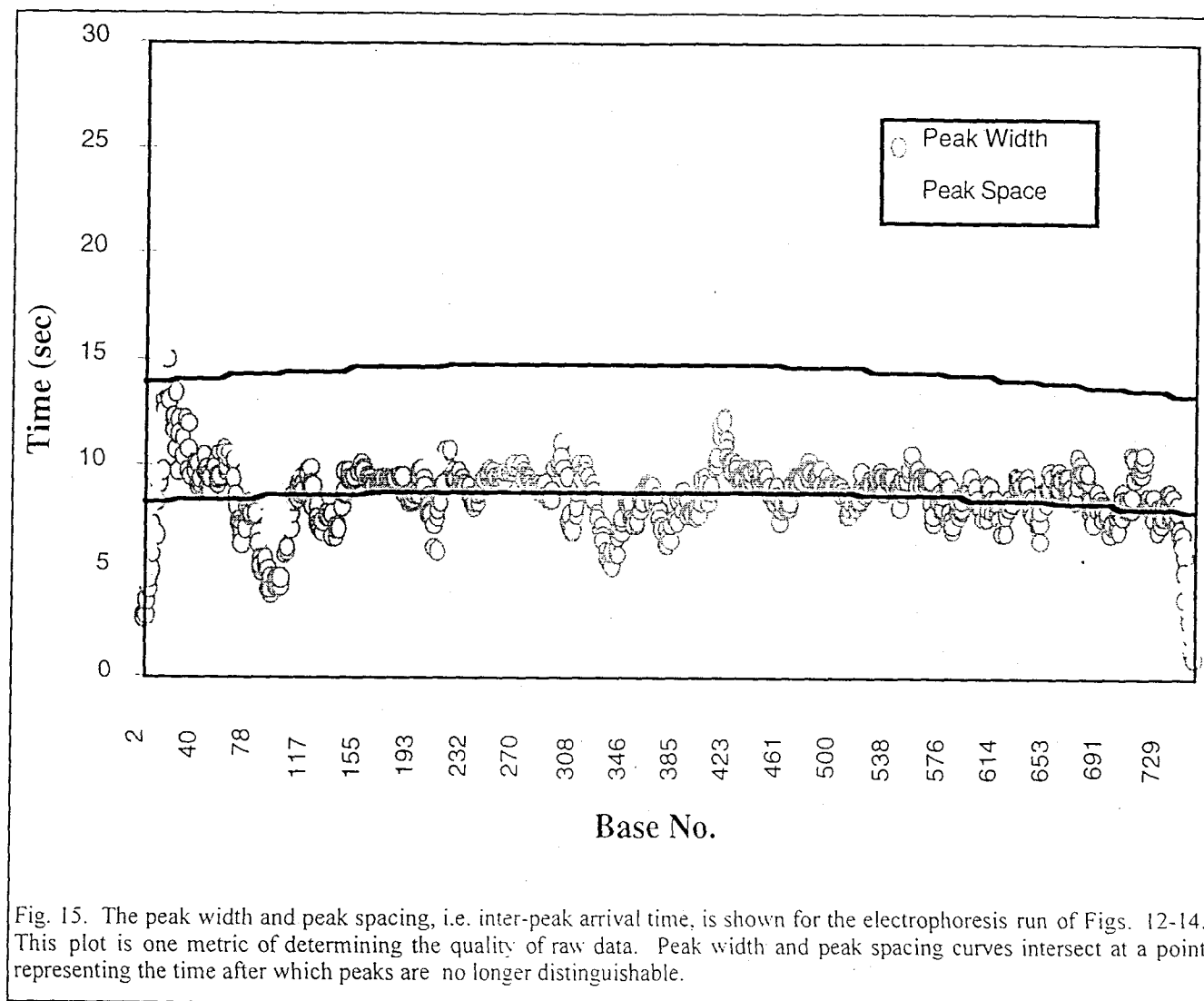


Fig. 15. The peak width and peak spacing, i.e. inter-peak arrival time, is shown for the electrophoresis run of Figs. 12-14. This plot is one metric of determining the quality of raw data. Peak width and peak spacing curves intersect at a point representing the time after which peaks are no longer distinguishable.

This work was performed under the auspices of the U.S. Department of Energy by Lawrence Livermore National Laboratory under contract No. W-7405-Eng-48.